Supporting Information

Mosaic structure effect and superior catalytic performance of $AgBr/Ag_2MoO_4$ composite materials

Jing-Yu Zhang, Yi Lu, Jin-Ku Liu*, Hao Jiang

Shanghai Key Laboratory of Multiphase Materials Chemical Engineering, School of Chemistry and Molecular Engineering, East China University of Science and Technology, Shanghai 200237 P.R. China

* **Corresponding author; E-mail address:** jkliu@ecust.edu.cn

Characterizations

The structures of Ag_2MoO_4 and AgBr-Ag_2MoO_4 composite materials (CMs) were characterized by X-ray powder diffraction (XRD) (Cu *Kα* radiation) using a Shimadzu XD-3A diffractometer. The microstructures and morphologies were analyzed by scanning electron microscopy (SEM, Philips S-4800). Philips S-4800 energy disperse spectroscopy (EDS) was measured to study the surface composition. The optical properties of the products were studied by the Fourier conversion infrared spectroscopy (FT-IR). The UV-Vis spectroscopy (Shimadzu, UV-2450) was measured to explore the absorption properties of products. The surface composition of product was researched by X-ray photoelectron spectroscopy (XPS, VG ESCALAB MK Ⅱ). The special surface area (BET) was determined by isothermal nitrogen adsorption-desorption analysis (Micromeritics ASAP 2400).

S1. Morphologies and composition of AgX-Ag_2MoO_4 (X = Cl, Br, I) catalysts

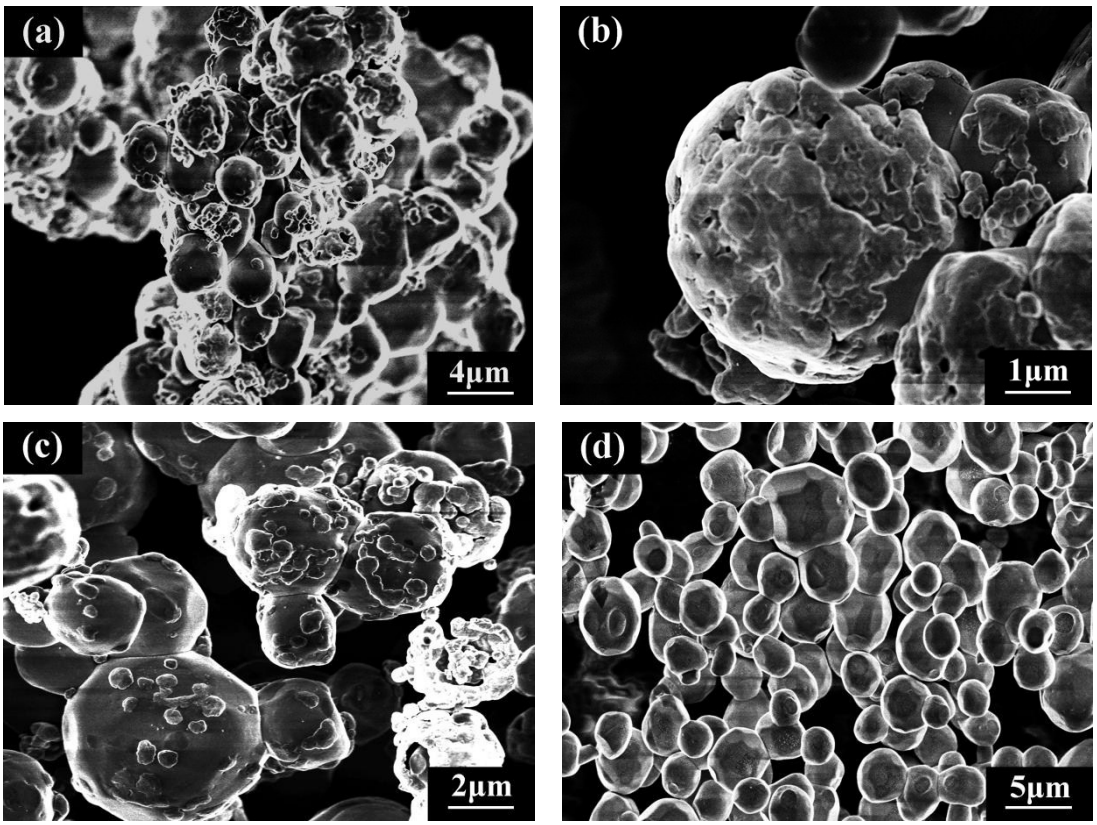

Figure S1. The SEM patterns of (a) AgCl-Ag_2MoO_4; (b) AgBr-Ag_2MoO_4; (c) AgI-Ag_2MoO_4; (d) Ag_2MoO_4 (6h)

S2. The TEM images of the samples melting process

We have tried the TEM test. Unfortunately, the sample could not suffer the thermal radiation from electron beam. When the electron beam focus on the sample, the extreme heat would melt the sample and damage it instantly. Therefore we could not get the clear TEM images which had the details of the sample. The failing TEM images were showed in Figure S2.

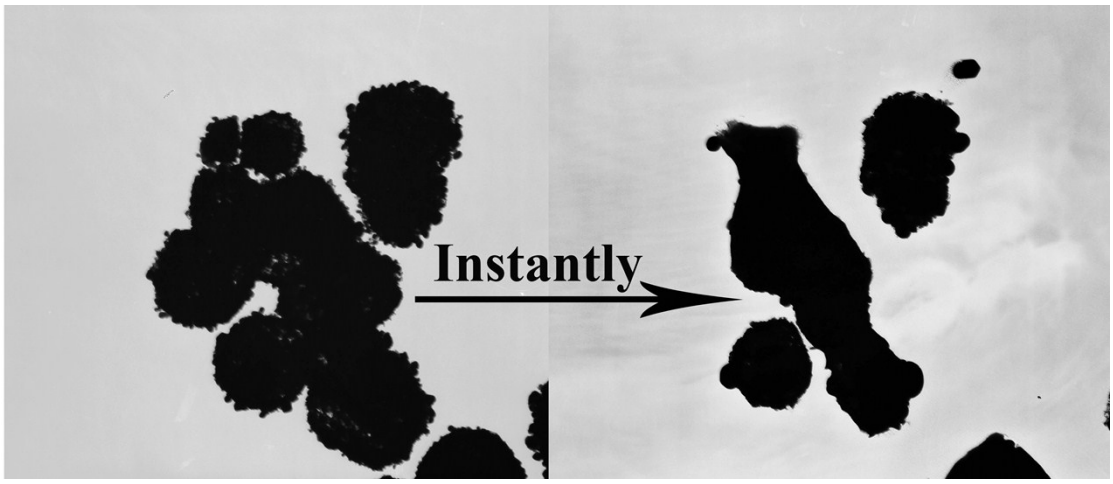

Figure S2. The TEM images of the samples melting process.

S3. Optical properties of AgX-Ag_2MoO_4 (X = Cl, Br, I) catalysts

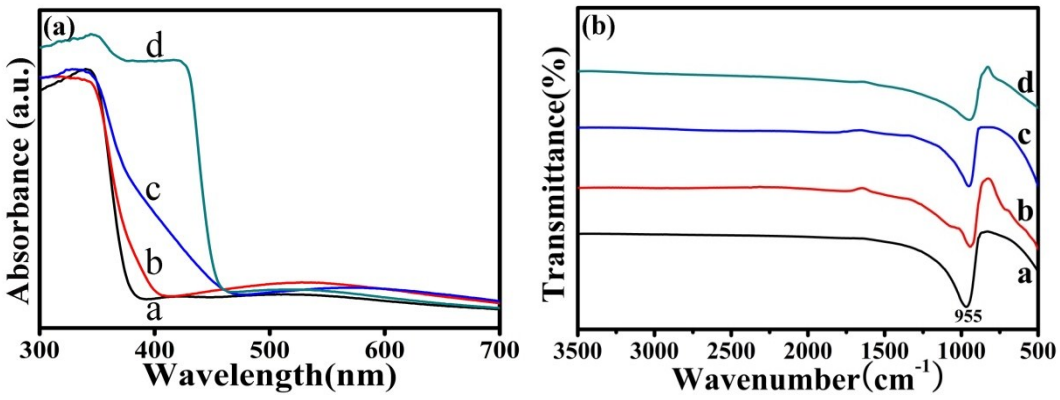

Figure S3. (a) UV-Vis absorption spectra and (b) FT-IR spectra of different catalyst: a

Ag_2MoO_4; b AgCl-Ag_2MoO_4; c AgBr-Ag_2MoO_4; d AgI-Ag_2MoO_4

UV-visible absorption spectra were shown in Figure S3(a), which presented AgX-Ag_2MoO_4 CMs absorption and pure Ag_2MoO_4 absorption spectrum at the same coordinate axis. It indicated that pure Ag_2MoO_4 had no absorption in the visible region, whereas the AgX-Ag_2MoO_4 CMs had a significantly performance in visible-light absorption. When Ag_2MoO_4 was composited with AgCl, the absorption in the visible area enhanced with a certain degree, but not dramatically. When it came to AgBr, it was clear that the absorption in the visible region had been broaden to 450 nm. However, the AgI-Ag_2MoO_4 CMs had a certain performance in the ultraviolet area. The results meant that more efficient absorption overlap with the solar spectrum after compositing AgX with Ag_2MoO_4. The FT-IR spectra of the pure Ag_2MoO_4 and AgX-Ag_2MoO_4 CMs were presented in Figure S3(b). The characteristic peak at 955 cm^{-1} was assigned to the stretching vibration of O-Mo-O.

S4. Adsorption equilibrium experiment of the catalysts

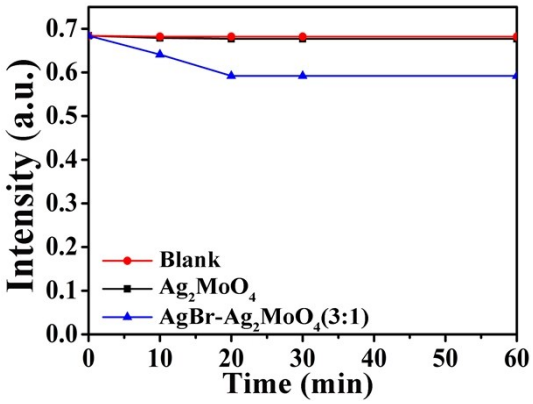

Figure S4. The adsorption capacity of obtained samples in dark environment

S5. Photocatalytic performance of AgX-Ag_2MoO_4 (X = Cl, Br, I) catalysts on degrading Rh. B

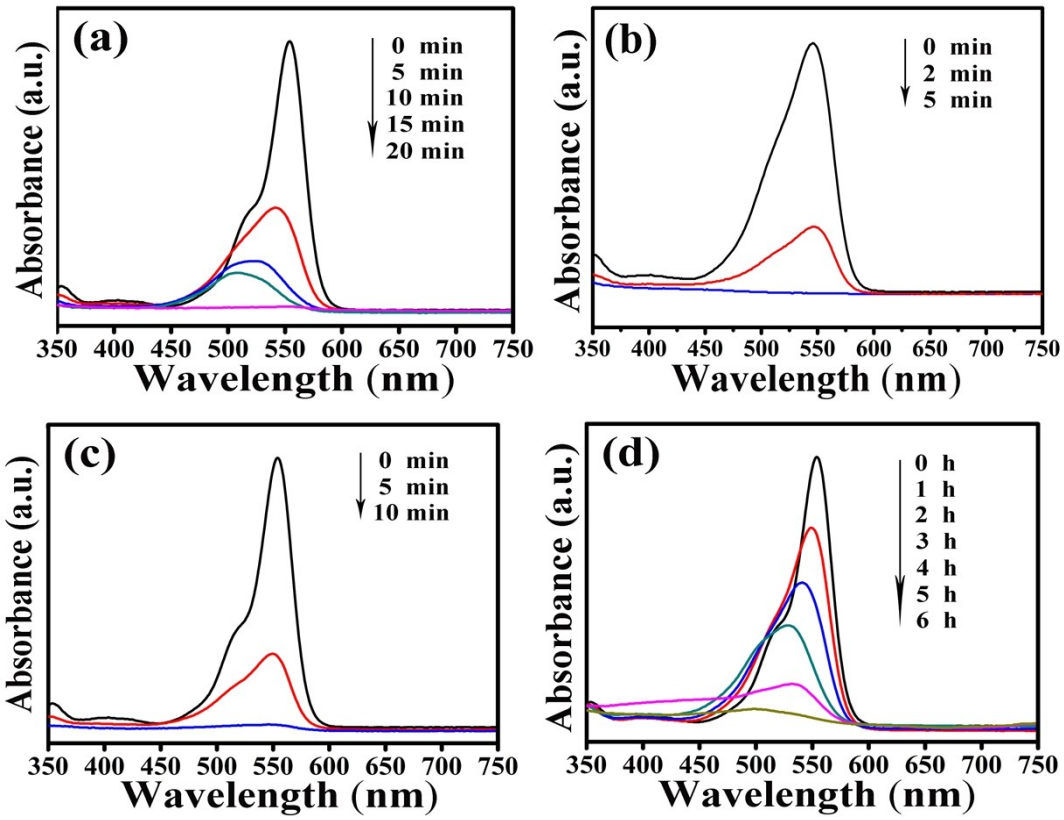

Figure S5. The photocatalytic degradation curves of AgX-Ag_2MoO_4 CMs and pure Ag_2MoO_4 to the Rh.B dyes under the irradiation of 500 W mercury lamp (a) AgCl-Ag_2MoO_4 (1:1); (b) AgBr-Ag_2MoO_4 (1:1); (c) AgI-Ag_2MoO_4 (1:1); (d) Ag_2MoO_4

S6. The cyclic degradation patterns of AgBr-Ag_2MoO_4 to the Rh.B dyes

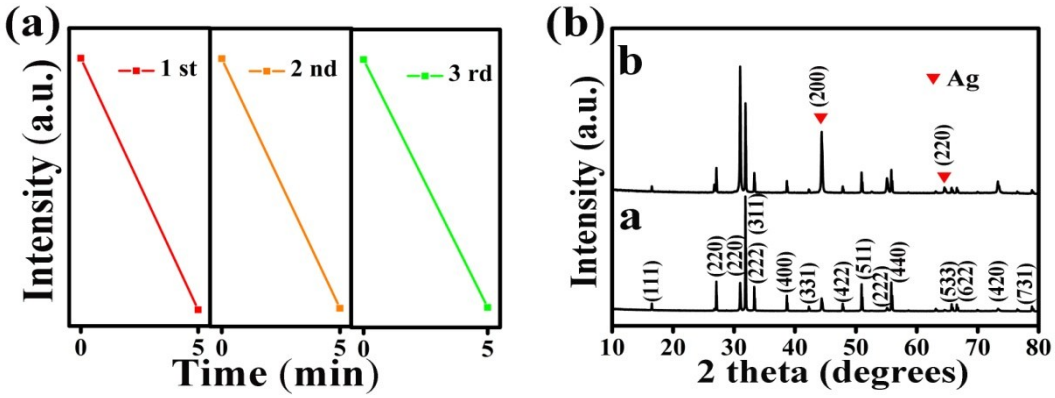

Figure S6. (a) The cyclic degradation patterns of AgBr-Ag_2MoO_4 to the Rh.B dyes under the irradiation of 500 W mercury lamp (b) The XRD patterns of the AgBr-Ag_2MoO_4: a fresh; b recycling process

The good performance ensured the application of AgBr-Ag_2MoO_4 CMs under UV irradiation. The standard of applied photocatalysts included not only the high photocatalytic activity but also the good photostability. Hence, the durability of AgBr-Ag_2MoO_4 CMs was studied and the recycle curves were shown in Figure S6a, where the declining efficiency of AgBr-Ag_2MoO_4 CMs reduced from 100 % (first run) to 92.7% (third run) under UV light within 5 min. The good stability of AgBr-Ag_2MoO_4 CMs under UV light was beneficial to the application in treating wastewater. The possible reason for the decrease of photocatalytic performance was about the losses in the process of operation. After recycling 3 times, the catalyst samples were analyzed by XRD. The diffraction peaks of 44 and 64 degree corresponded to the (200), and (220) crystal face which matched with the Ag cubic crystal system. The result indicated that negligible amounts of Ag element were generated under the strong UV light irradiation. However, these little Ag^0 have precisely contributed to the photocatalytic reaction. Therefore, the AgBr-Ag_2MoO_4 CMs, as novel catalysts, had good stability and great potential in practical application.

S7. Photocatalytic performance of AgBr-Ag_2MoO_4 (X = Cl, Br, I) catalysts on degrading phenol

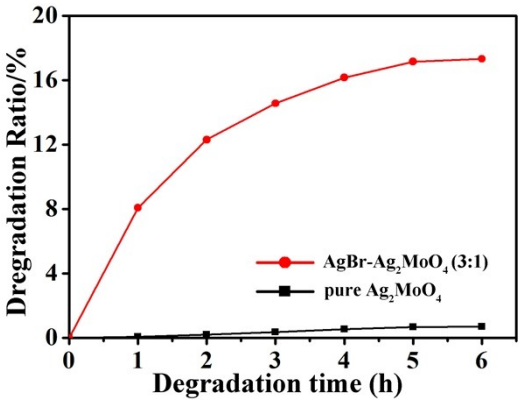

Figure S7. Degradation of phenol by AgBr-Ag_2MoO_4 CMs and the pure Ag_2MoO_4

To further demonstrate the photocatalytic degradation ability of AgBr-Ag_2MoO_4 CMs for colorless organic pollutants like phenol, photoreactions were carried out under UV light. The 0.05 g 3AgBr-Ag_2MoO_4 (the molar ratio was 3:1) CMs and pure Ag_2MoO_4 were added into the phenol solution (100 mg/L) respectively. Figure S7 showed that it was hard for the 3AgBr-Ag_2MoO_4 CMs and the pure Ag_2MoO_4 to degrade the phenol completely within 6 h. However, it is worth pointing out that the photocatalytic activity of 3AgBr-Ag_2MoO_4 CMs was still higher than pure Ag_2MoO_4 under the same condition. It was found that 17.32 % of phenol was decomposed within 6 h by 3AgBr-Ag_2MoO_4 CMs comparing 0.7 % in the case of pure Ag_2MoO_4. The results indicated that the AgBr-Ag_2MoO_4 catalyst could selectively degrade the organics.

S8. Mechanism of degradation of Rh. B under visible light

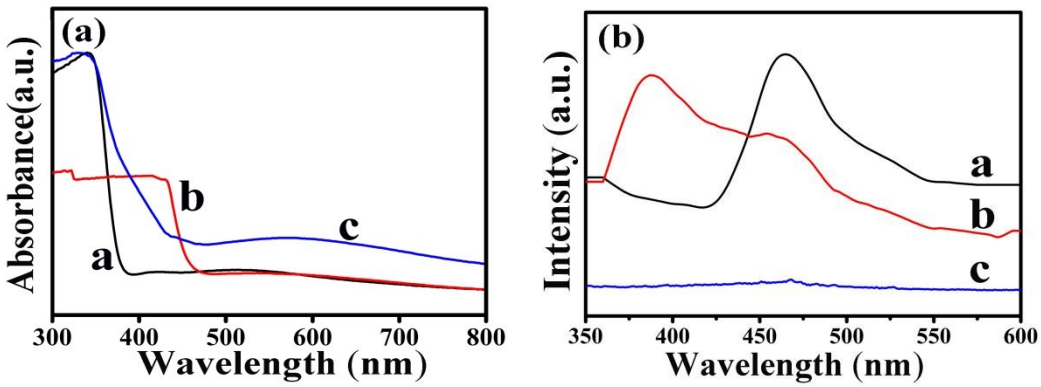

Figure S8. (a) UV-Vis absorption spectra and (b) the fluorescence spectra of a Ag_2MoO_4; b AgBr; c AgBr-Ag_2MoO_4

The properties of AgBr，Ag_2MoO_4，and AgBr-Ag_2MoO_4 CMs were characterized by UV-Vis absorption spectra and fluorescence spectra in order to

explore the reason why AgBr-Ag_2MoO_4 CMs performed outstanding photocatalytic activity. AgBr, Ag_2MoO_4 and AgBr-Ag_2MoO_4 CMs had strong absorption in the ultraviolet region, while the absorption spectra of AgBr and AgBr-Ag_2MoO_4 CMs were wider than Ag_2MoO_4 (Figure S8). Therefore, Ag_2MoO_4 had relatively poor photocatalytic efficiency. The ultraviolet absorption intensity of AgBr was obviously weaker than AgBr-Ag_2MoO_4 CMs. Also, the photoresponse performance of AgBr-Ag_2MoO_4 CMs was the best among these three materials in visible region. There was another distinct absorption peak located at the range of 470-600 nm which due to the surface plasmon resonance (SPR) absorption peak of the metal Ag. The conclusion was that the composite material had better light adsorption ability than monomer material.

Figure S8(b) was photoluminescence spectra of the above materials at an excitation wavelength of 320 nm under the room temperature. Mutual recombination of electrons and holes would release energy in the fluorescence spectra. So the lower fluorescence intensity of electrons and holes illustrated the lower recombination rate. On account of the fact that the photocatalytic properties and the effective separation of electrons and holes had a close relationship, the lower fluorescence intensity of material led to the better photocatalytic performance. The fluorescence intensity of AgBr and Ag_2MoO_4 was stronger than AgBr-Ag_2MoO_4 CMs. The heterostructure complex of AgBr and Ag_2MoO_4 can promote separation of electrons and holes to a great extent, which helped to improve the efficiency of photocatalysis.